



Chapter 16

Vanuatu

The contributions of Salesa Kaniaha and Philip Malsale from the Vanuatu Meteorology and Geo-hazard Department are gratefully acknowledged

Introduction

This chapter provides a brief description of Vanuatu, its past and present climate as well as projections for the future. The climate observation network and the availability of atmospheric and oceanic data records are outlined. The annual mean climate, seasonal cycles and the influences of large-scale climate features such as the South Pacific Convergence Zone and patterns of climate variability

(e.g. the El Niño-Southern Oscillation) are analysed and discussed. Observed trends and analysis of air temperature, rainfall, extreme events (including tropical cyclones), sea-surface temperature, ocean acidification, mean and extreme sea levels are presented. Projections for air and sea-surface temperature, rainfall, sea level, ocean acidification and extreme events for the 21st century are provided.

These projections are presented along with confidence levels based on expert judgement by Pacific Climate Change Science Program (PCCSP) scientists. The chapter concludes with a summary table of projections (Table 16.4). Important background information including an explanation of methods and models is provided in Chapter 1. For definitions of other terms refer to the Glossary.

16.1 Climate Summary

16.1.1 Current Climate

- Temperatures in the warmest months in Vanuatu (January-February) are about 4°C higher than those in the coolest months (July-August).
- Vanuatu has a marked wet season from November to April.
- Vanuatu's rainfall is strongly influenced by the position and strength of the South Pacific Convergence Zone. During summer the South Pacific Convergence Zone intensifies and moves further south, bringing the higher rainfall of the wet season.
- Rainfall in Vanuatu varies greatly from year-to-year due mainly to the influence of the El Niño-Southern Oscillation.
- Warming trends are evident in both annual and seasonal mean air temperatures for Bauerfield Airport (Port Vila) for the period 1950–2009.

- The sea-level rise near Vanuatu measured by satellite altimeters since 1993 is about 6 mm per year.
- Annual and seasonal rainfall trends for Port Vila and Aneityum for the period 1950–2009 are not statistically significant.
- On average Port Vila experiences 23 tropical cyclones per decade, with most occurring in January and February. The high interannual variability in tropical cyclone numbers makes it difficult to identify any long-term trends in frequency.

16.1.2 Future Climate

Over the course of the 21st century:

- Surface air temperature and sea-surface temperature are projected to continue to increase (*very high* confidence).
- Wet season rainfall is projected to increase (*moderate* confidence).
- Dry season rainfall is projected to decrease (*moderate* confidence).

- Little change is projected in annual mean rainfall (*low* confidence).
- The intensity and frequency of days of extreme heat are projected to increase (*very high* confidence).
- The intensity and frequency of days of extreme rainfall are projected to increase (*high* confidence).
- Little change is projected in the incidence of drought (*low* confidence).
- Tropical cyclone numbers are projected to decline in the south-west Pacific Ocean basin (0–40°S, 130°E –170°E) (*moderate* confidence).
- Ocean acidification is projected to continue (*very high* confidence).
- Mean sea-level rise is projected to continue (*very high* confidence).

16.2 Country Description

The island archipelago of Vanuatu lies between 13°S–21°S and 166°E–171°E and includes over 80 islands. The largest island is Espiritu Santo while the island of Efate is home to the capital, Port Vila and the Vanuatu Government. Vanuatu has an Economic Exclusion Zone of 710 000 km² which encompasses Vanuatu's total land area of 12 190 km². Larger islands

are characterised by rugged volcanic peaks and tropical rainforests. The highest peak, Mount Tabwemasana on Espiritu Santo, is 1877 m above mean sea level.

Vanuatu's population in 2009 was estimated at 234 023 of which around 80% live in rural areas (Vanuatu Country Profile, SOPAC, 2000; Vanuatu National Statistics Office, 2010).

Most of Vanuatu's population relies on subsistence agriculture. Cocoa, copra and coffee exports contribute to Vanuatu's economy alongside tourism, logging and fishing. Revenue from mineral extraction is relatively new to the economy and may provide significant revenue in the future (Vanuatu Country Profile, SOPAC, 2000).

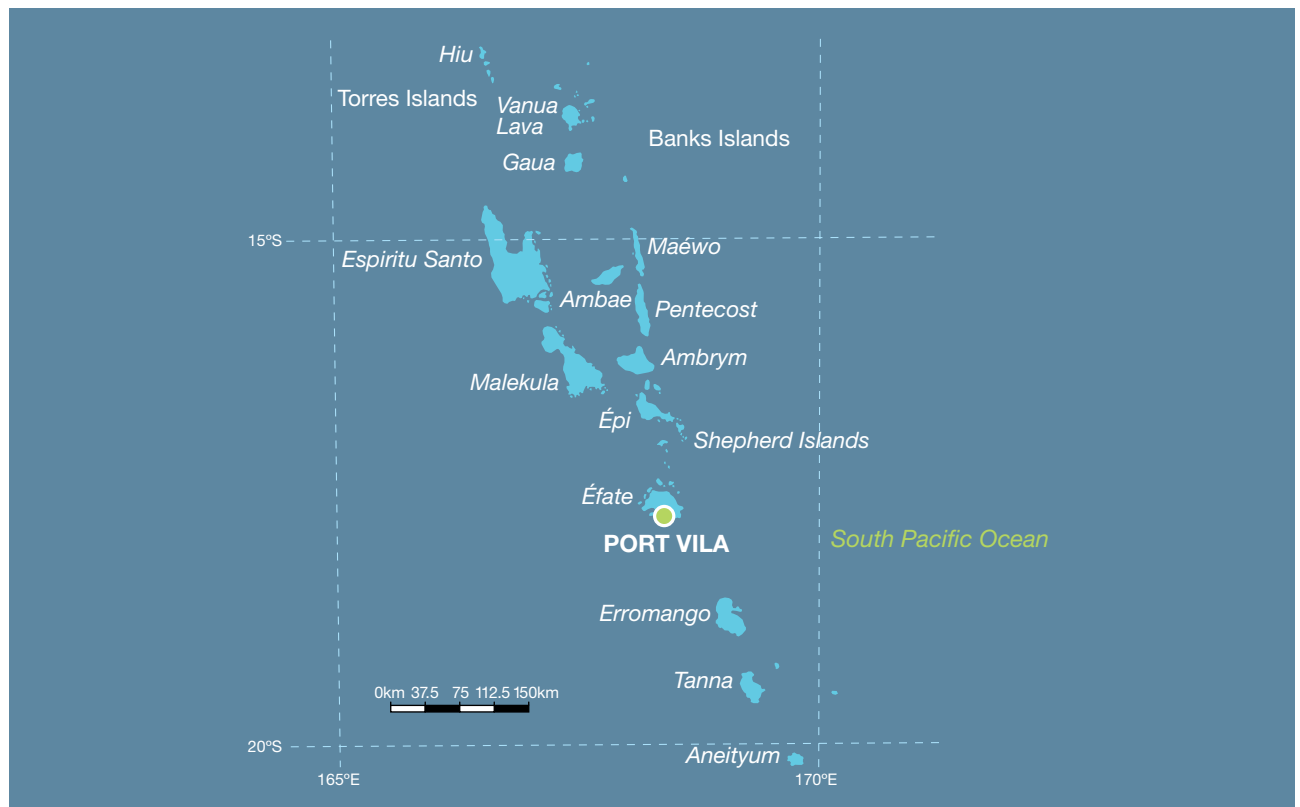


Figure 16.1: Vanuatu

16.3 Data Availability

There are currently 47 operational meteorological stations in Vanuatu. Multiple observations within a 24-hour period are taken at Sola, Pekoa, Saratamata, Lamap, Bauerfield, Whitegrass and Analguahat. At three climate stations, Lambubu, Lamap and Aneityum, and at 39 rainfall stations across the country a single observation is taken daily at 9.00 am local time. The primary climate stations are located at Port Vila and Bauerfield Airport on the island of Efate (Figure 16.1). Several stations, including Iririki (Port Vila), have rainfall data from the early 1900s. Iririki also has the earliest air temperature observations which began in the late 1940s.

Records used include a composite Iririki-Vila rainfall record, composite air temperature Iririki-Vila-Bauerfield record and single site record from Aneityum (southern Vanuatu) for the period 1950–2009.

The Iririki-Vila-Bauerfield and Aneityum records are homogeneous and more than 95% complete.

Oceanographic records do not cover such a long time period. Monthly-averaged sea-level data are available from Port Vila (1993–present). A global positioning system instrument to estimate vertical land motion was deployed at Port Vila in 2002 and will provide valuable direct estimates of local vertical land motion in future

years. Both satellite (from 1993) and in situ sea-level data (1950–2009; termed reconstructed sea level; Volume 1, Section 2.2.2.2) are available on a global $1^\circ \times 1^\circ$ grid.

Long-term locally-monitored sea-surface temperature data are unavailable for Vanuatu, so large-scale gridded sea-surface temperature datasets have been used (HadISST, HadSST2, ERSST and Kaplan Extended SST V2; Volume 1, Table 2.3).



Climate data management training, Vanuatu Meteorology and Geo-hazard Department

16.4 Seasonal Cycles

The seasonal variations in rainfall and air temperature at both Port Vila (in the central region of Vanuatu) and Aneityum (in the south) are very similar (Figure 16.2). Being further south, mean monthly Aneityum temperatures are about 2°C cooler than those in Port Vila. Both sites have highest temperatures in January-February, with the coolest months (July-August) about 4°C cooler than the warmest months. The cooler winter air temperatures are due to weaker solar radiation and the influence of high pressure cells bringing cold winds from higher latitudes. Seasonal variations in sea-surface temperatures closely

match those of air temperatures and have a strong influence on the air temperatures on the islands of Vanuatu.

Both sites have a marked wet season from November to April, with highest rainfall from January to March, and a dry season from May to October. The difference between seasons is slightly more marked in Port Vila as Aneityum receives more rainfall from extra-tropical influences such as cold fronts during the dry season. Vanuatu's rainfall is strongly influenced by the position and strength of the South Pacific Convergence Zone

(SPCZ), which lies north of the country during the winter. During summer the SPCZ intensifies and moves further south, bringing the higher rainfall of the wet season. Low pressure systems embedded in the SPCZ often become tropical cyclones during the cyclone season. Topography also plays a role in the variations in rainfall across some islands. During the wet season, rainfall is particularly high on the windward (south-east) side of the mountain ranges of the bigger islands, and scarce during the dry season, especially on the leeward (north-west) sides.

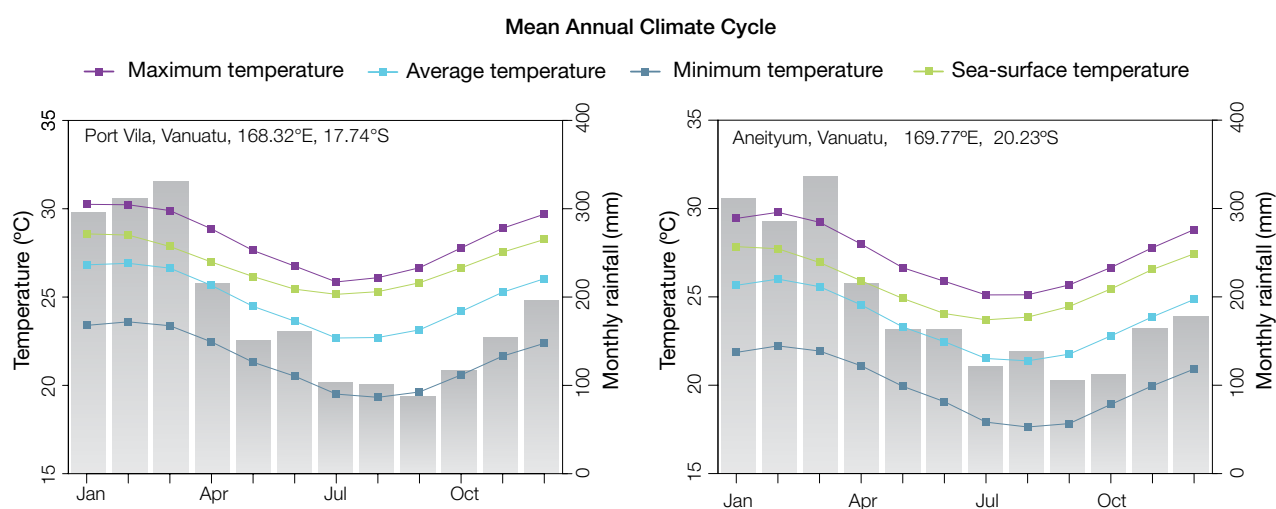


Figure 16.2: Mean annual cycle of rainfall (grey bars) and daily maximum, minimum and mean air temperatures at Port Vila (left) and Aneityum (right), and local sea-surface temperatures derived from the HadISST dataset (Volume 1, Table 2.3).

16.5 Climate Variability

Large variations in rainfall are observed in Vanuatu from year-to-year (Figure 16.4). The wettest years receive up to three times more than the driest years. Much of this variability is linked to the El Niño-Southern Oscillation (ENSO). There are significant correlations between ENSO indices and both rainfall and air temperature in Vanuatu (Tables 16.1 and 16.2). The impact of ENSO on climate in Port Vila and Aneityum are similar: El Niño events tend to bring a late start to the wet season and lower rainfall in both the wet and dry seasons, as well as cooler conditions in the dry season. Opposite impacts are usually observed during La Niña events. ENSO Modoki events (Volume1, Section 3.4.1) are as important as canonical ENSO events in Port Vila, and have much the same impacts, but are less influential further south in Aneityum. Long-term ENSO variability, seen in the Interdecadal Pacific Oscillation, appears to have a weak but significant influence on decadal rainfall variability in Port Vila during the dry season.

Table 16.1: Correlation coefficients between indices of key large-scale patterns of climate variability and minimum and maximum temperatures (Tmin and Tmax) and rainfall at Port Vila. Only correlation coefficients that are statistically significant at the 95% level are shown.

Climate feature/index		Dry season (May-October)			Wet season (November-April)		
		Tmin	Tmax	Rain	Tmin	Tmax	Rain
ENSO	Niño3.4	-0.41	-0.41	-0.45			-0.49
	Southern Oscillation Index	0.36	0.41	0.36			0.51
Interdecadal Pacific Oscillation Index				-0.28			
Southern Annular Mode Index							
ENSO Modoki Index		-0.40	-0.36	-0.26	-0.28		-0.45
Number of years of data		62	62	98	62	63	100

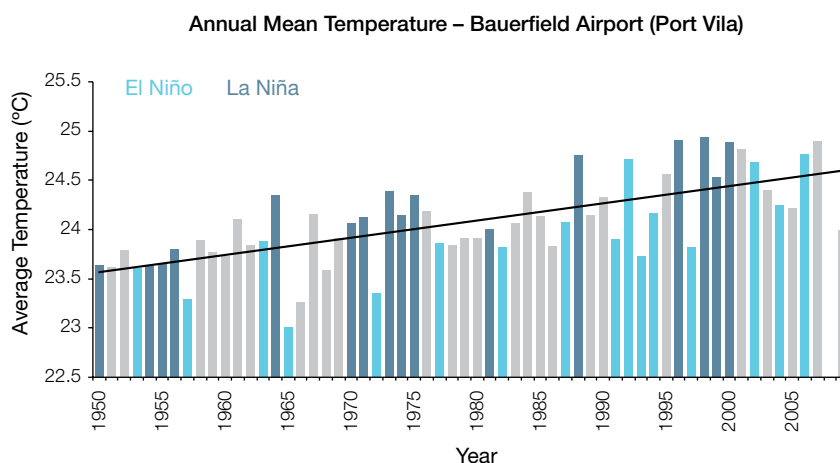
Table 16.2: Correlation coefficients between indices of key large-scale patterns of climate variability and minimum and maximum temperatures (Tmin and Tmax) and rainfall at Aneityum. Only correlation coefficients that are statistically significant at the 95% level are shown.

Climate feature/index		Dry season (May-October)			Wet season (November-April)		
		Tmin	Tmax	Rain	Tmin	Tmax	Rain
ENSO	Niño3.4	-0.51	-0.48	-0.43			-0.33
	Southern Oscillation Index	0.41	0.59	0.27			0.39
Interdecadal Pacific Oscillation Index							
Southern Annular Mode Index							
ENSO Modoki Index		-0.43	-0.45				
Number of years of data		59	58	61	55	53	60

16.6 Observed Trends

16.6.1 Air Temperature

Warming trends are evident in both annual and seasonal mean air temperatures at Bauerfield Airport (composite) and Aneityum for the period 1950–2009. Air temperature trends are stronger in the wet season when compared with the dry season, and minimum air temperature trends are stronger than maximum air temperature trends at both sites (Figure 16.3 and Table 16.3).



16.6.2 Rainfall

Annual and seasonal rainfall trends for Port Vila (composite) and Aneityum for the period 1950–2009 are not statistically significant (Table 16.3 and Figure 16.4).

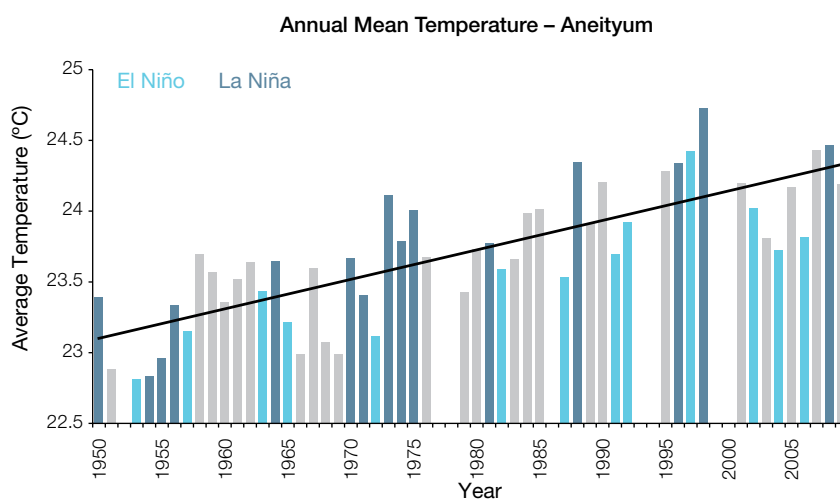


Figure 16.3: Annual mean air temperature at Bauerfield Airport (Port Vila) (top) and Aneityum (bottom). Light blue, dark blue and grey bars denote El Niño, La Niña and neutral years respectively.

Table 16.3: Annual and seasonal trends in maximum, minimum and mean air temperature (Tmax, Tmin and Tmean) and rainfall at Bauerfield Airport/Port Vila (composite) and Aneityum for the period 1950–2009. Asterisks indicate significance at the 95% level. Persistence is taken into account in the assessment of significance as in Power and Kociuba (in press). The statistical significance of the air temperature trends is not assessed.

	Bauerfield Airport Tmax (°C per 10 yrs)	Bauerfield Airport Tmin (°C per 10 yrs)	Bauerfield Airport Tmean (°C per 10 yrs)	Port Vila Rain (mm per 10 yrs)	Aneityum Tmax (°C per 10 yrs)	Aneityum Tmin (°C per 10 yrs)	Aneityum Tmean (°C per 10 yrs)	Aneityum Rain (mm per 10 yrs)
Annual	+0.17	+0.19	+0.17	-53	+0.18	+0.23	+0.21	-7
Wet season	+0.21	+0.21	+0.21	-40	+0.17	+0.25	+0.21	+4
Dry season	+0.13	+0.19	+0.15	-10	+0.16	+0.22	+0.19	-15

16.6.3 Extreme Events

The tropical cyclone season in the Vanuatu region is between November and April. Occurrences outside this period are rare. The tropical cyclone archive for the Southern Hemisphere indicates that between the 1969/70 and 2009/10 seasons, the centre of 94 tropical cyclones passed within approximately 400 km of Port Vila making this site the most impacted capital city in the PCCSP Partner Countries (Nuku'alofa, Tonga follows with 71 cyclones over the same period). This represents an average of 23 cyclones per decade. Tropical cyclone occurrence in El Niño, La Niña and neutral years are fairly similar (averages of 23, 25 and 22 cyclones per decade respectively). The interannual variability in the number of tropical cyclones in the vicinity of Port Vila is large, ranging from zero in some seasons to six in the 1971/72 season (Figure 16.5). This high variability makes it difficult to identify any long-term trends in frequency.

Impacts of climate variability and change are evident on most of Vanuatu's islands. ENSO-related drought and flooding are prevalent and continue to impact the socio-economic livelihood of the people of Vanuatu. For example, a flood event during the 2011 La Niña event washed through several villages on Emae Island, completely inundating agricultural land in Middle Bush, Tanna. Such occurrences are rare but the impacts can be devastating.

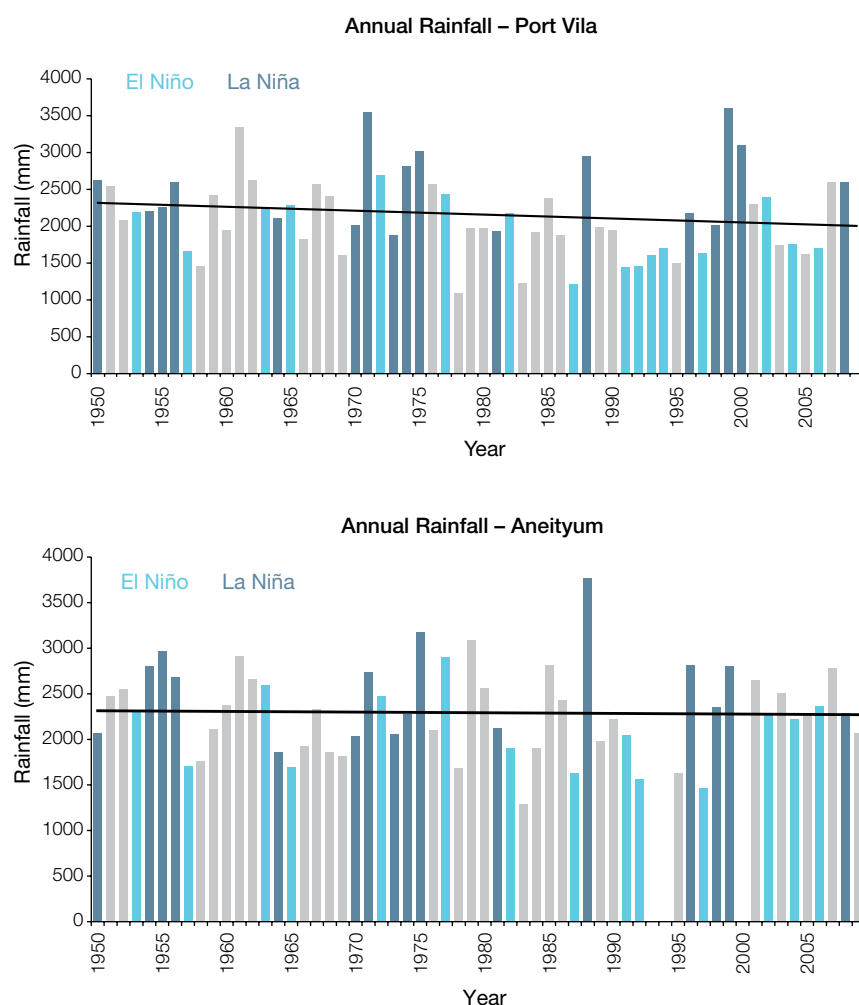


Figure 16.4: Annual rainfall at Port Vila (top) and Aneityum (bottom). Light blue, dark blue and grey bars denote El Niño, La Niña and neutral years respectively.

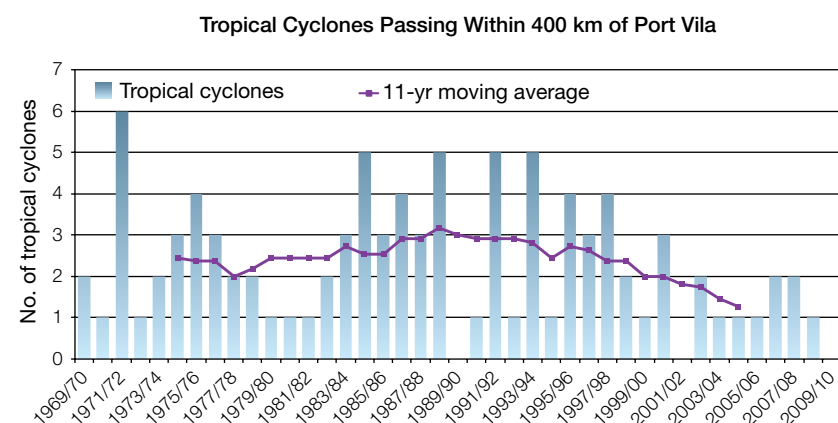


Figure 16.5: Tropical cyclones passing within 400 km of Port Vila per season. The 11-year moving average is in purple.

16.6.4 Sea-Surface Temperature

Historical changes around Vanuatu are consistent with the broad-scale sea-surface temperature changes of the PCCSP region. Water temperatures remained relatively constant from the 1950s to the late 1980s. This was followed by a period of more rapid warming (approximately 0.09°C per decade for 1970 to present). Figure 16.8 shows the 1950–2000 sea-surface temperature changes (relative to a reference year of 1990) from three different large-scale sea surface temperature datasets (HadSST2, ERSST and Kaplan Extended SST V2; Volume 1, Table 2.3). At these regional scales, natural variability may play a large role in the sea-surface temperature changes making it difficult to identify any long-term trends.

16.6.5 Ocean Acidification

Based on the large-scale distribution of coral reefs across the Pacific and the seawater chemistry, Guinotte et al. (2003) suggested that seawater aragonite saturation states above 4 were optimal for coral growth and for the development of healthy reef ecosystems, with values from 3.5 to 4 adequate for coral growth, and values between 3 and 3.5, marginal. Coral reef ecosystems were not found at seawater aragonite saturation states below 3 and these conditions were classified as extremely marginal for supporting coral growth.

In the Vanuatu region, the aragonite saturation state has declined from about 4.5 in the late 18th century to an observed value of about 3.9 ± 0.1 by 2000.

16.6.6 Sea Level

Monthly averages of the historical tide gauge, satellite (since 1993) and gridded sea-level (since 1950) data agree well after 1993 and indicate interannual variability in sea levels of about 18 cm (estimated 5–95% range) after removal of the seasonal cycle (Figure 16.10). The sea-level rise near Vanuatu measured by satellite altimeters (Figure 16.6) since 1993 is about 6 mm per year, larger than the global average of 3.2 ± 0.4 mm per year. This rise is partly linked to a pattern related to climate variability from year to year and decade to decade (Figure 16.10).

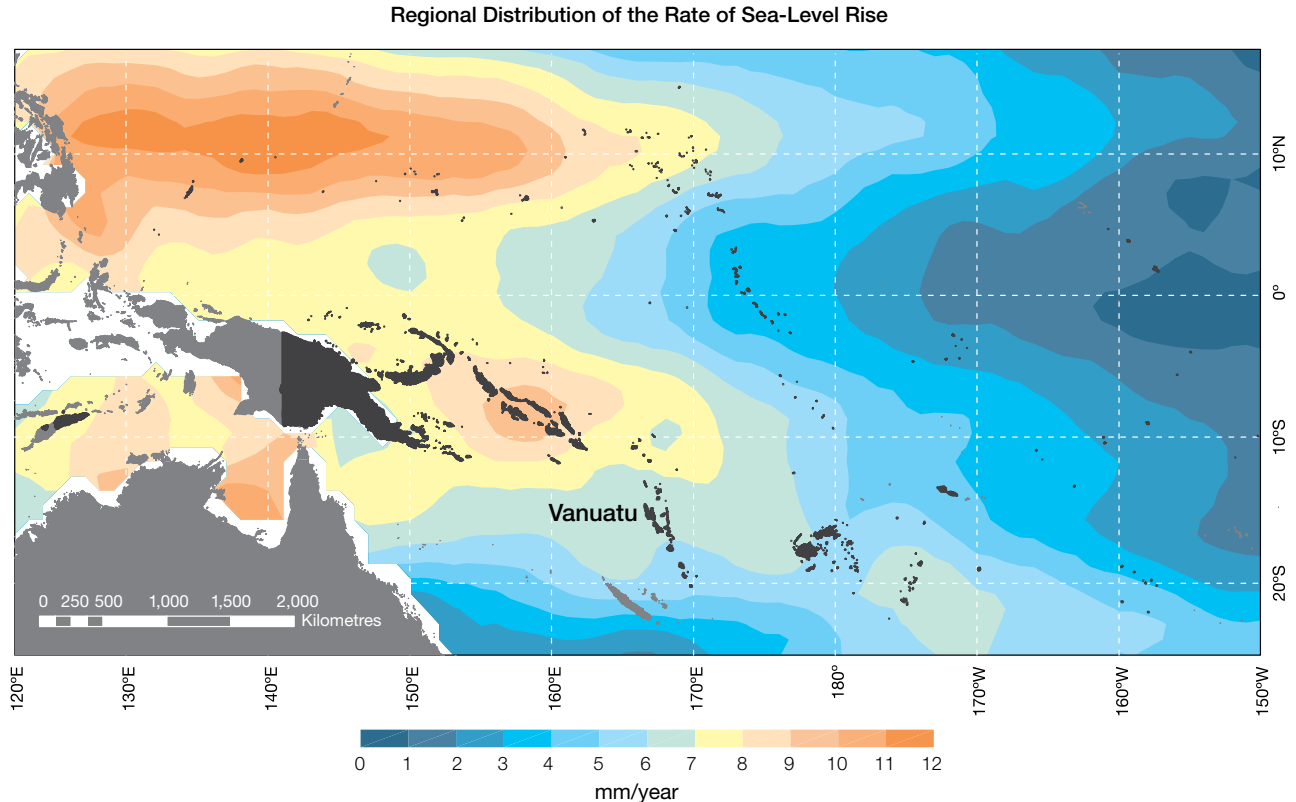


Figure 16.6: The regional distribution of the rate of sea-level rise measured by satellite altimeters from January 1993 to December 2010, with the location of Vanuatu indicated. Further detail about the regional distribution of sea-level rise is provided in Volume 1, Section 3.6.3.2.

16.6.7 Extreme Sea-Level Events

The annual climatology of the highest daily sea levels has been evaluated from hourly measurements by the tide gauge at Port Vila (Figure 16.7). High tides peak in November to January. Seasonal variations throughout the year are small. However, seasonal

water levels tend to be higher during La Niña years and slightly lower during El Niño years (Volume 1, Section 3.6.3 and Figures 3.20 and 3.21). Short-term variations show evidence of a seasonal cycle, with a generally higher likelihood of high water levels in December to March, roughly corresponding to the cyclone season. ENSO does not strongly affect short-term water level

events. These tidal, seasonal and short-term components combine to produce a highest likelihood of extreme water levels from October through March. The top 10 water level events mostly occurred within this time frame during La Niña or ENSO-neutral conditions. Several were associated with a cyclone or tropical disturbance in the vicinity.

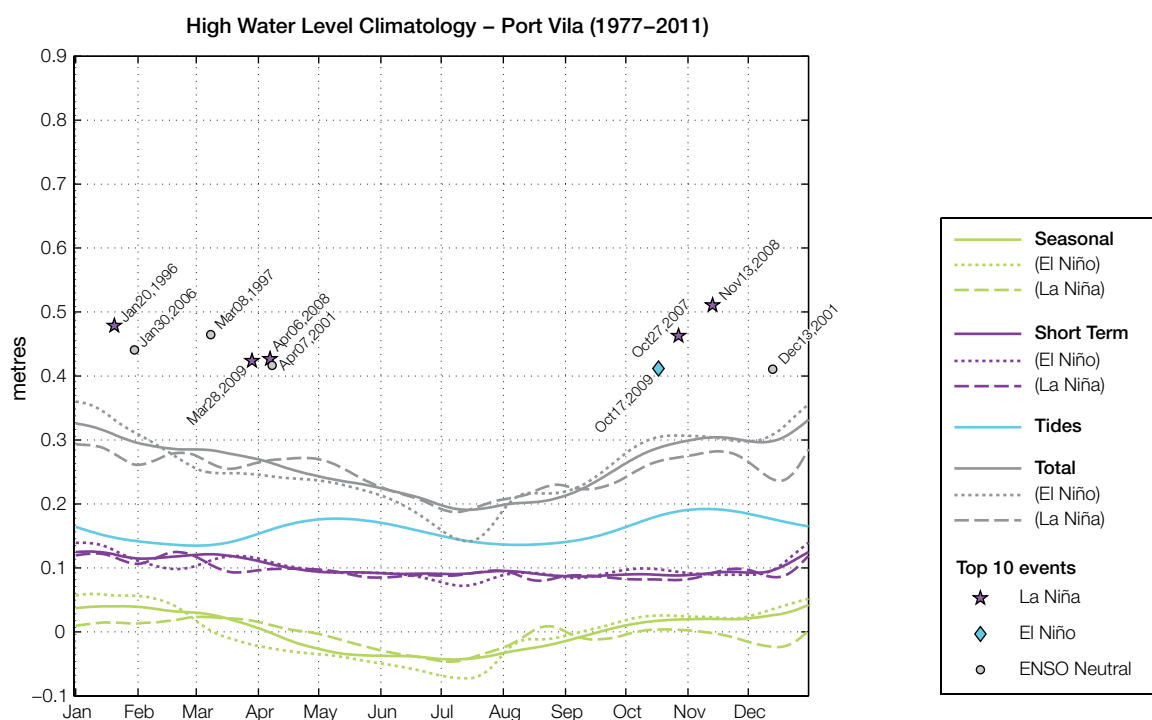


Figure 16.7: The annual cycle of high waters relative to Mean Higher High Water (MHHW) due to tides, short-term fluctuations (most likely associated with storms) and seasonal variations for Port Vila. The tides and short-term fluctuations are respectively the 95% exceedence levels of the astronomical high tides relative to MHHW and short-term sea-level fluctuations. Components computed only for El Niño and La Niña months are shown by dotted and dashed lines, and grey lines are the sum of the tide, short-term and seasonal components. The 10 highest sea-level events in the record relative to MHHW are shown and coded to indicate the phase of ENSO at the time of the extreme event.

16.7 Climate Projections

Climate projections have been derived from up to 18 global climate models from the CMIP3 database, for up to three emissions scenarios (B1 (low), A1B (medium) and A2 (high)) and three 20-year periods (centred on 2030, 2055 and 2090, relative to 1990). These models were selected based on their ability to reproduce important features of the current climate (Volume 1, Section 5.2.3), so projections arising from each of the models are plausible representations of the future climate. This means there is not one single projected future for Vanuatu, but rather a range of possible futures. The full range of these futures is discussed in the following sections.

These projections do not represent a value specific to any actual location, such as a town or city in Vanuatu. Instead, they refer to an average change over the broad geographic region encompassing the islands of Vanuatu and the surrounding ocean (Figure 1.1 shows the regional boundaries). Section 1.7 provides important information about interpreting climate model projections.

16.7.1 Temperature

Surface air temperature and sea-surface temperature are projected to continue to increase over the course of the 21st century. There is *very high* confidence in this direction of change because:

- Warming is physically consistent with rising greenhouse gas concentrations.
- All CMIP3 models agree on this direction of change.

The majority of CMIP3 models simulate a slight increase ($<1^{\circ}\text{C}$) in annual and seasonal mean temperature by 2030, however by 2090 under the A2 (high) emissions scenario temperature increases of greater than 2.5°C are simulated by almost all models (Table 16.4). Given the close relationship between surface air temperature and sea-surface temperature, a similar (or slightly

weaker) rate of warming is projected for the surface ocean (Figure 16.8). There is *high* confidence in this range and distribution of possible futures because:

- There is generally close agreement between modelled and observed temperature trends over the past 50 years in the vicinity of Vanuatu, although observational records are limited (Figure 16.8).

Interannual variability in surface air temperature and sea-surface temperature over Vanuatu is strongly influenced by ENSO in the current climate (Section 16.5). As there is no consistency in projections of future ENSO activity (Volume 1, Section 6.4.1) it is not possible to determine whether interannual variability in temperature will change in the future. However, ENSO is expected to continue to be an important source of variability for the region.

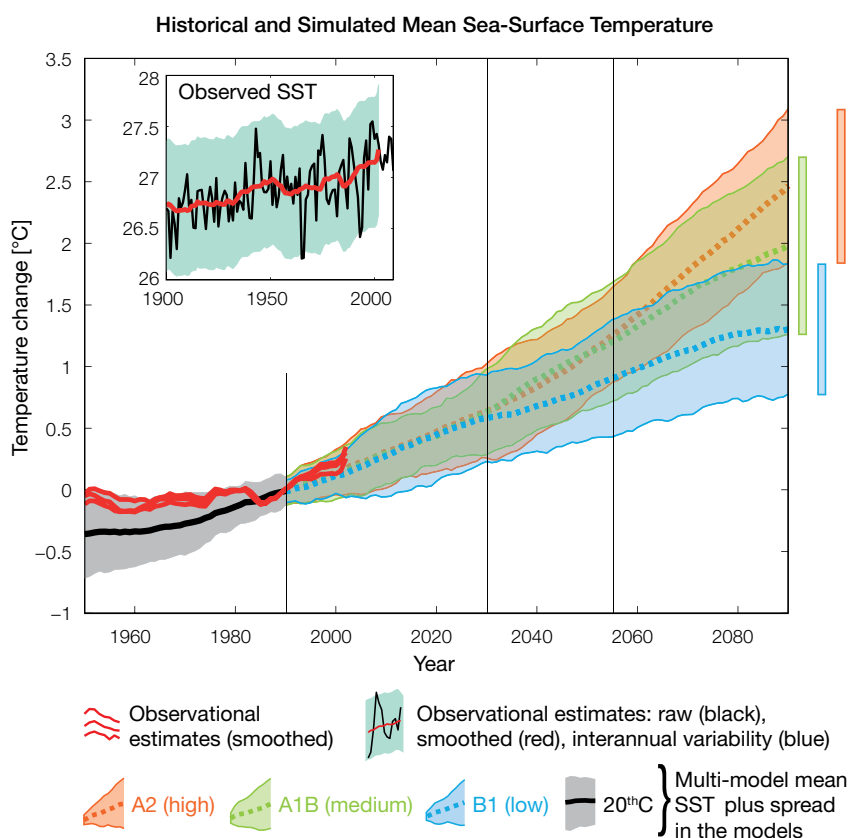


Figure 16.8: Historical climate (from 1950 onwards) and simulated historical and future climate for annual mean sea-surface temperature (SST) in the region surrounding Vanuatu, for the CMIP3 models. Shading represents approximately 95% of the range of model projections (twice the inter-model standard deviation), while the solid lines represent the smoothed (20-year running average) multi-model mean temperature. Projections are calculated relative to the 1980–1999 period (which is why there is a decline in the inter-model standard deviation around 1990). Observational estimates in the main figure (red lines) are derived from the HadSST2, ERSST and Kaplan Extended SST V2 datasets (Volume 1, Section 2.2.2). Annual average (black) and 20-year running average (red) HadSST2 data is also shown inset.

16.7.2 Rainfall

Wet Season (November–April)

Wet season rainfall is projected to increase over the course of the 21st century. There is *moderate* confidence in this direction of change because:

- An increase in wet season rainfall is consistent with the projected likely increase in the intensity of the South Pacific Convergence Zone (SPCZ), which lies over Vanuatu in this season (Volume 1, Section 6.4.5).
- The majority of CMIP3 models agree on this direction of change by 2090.

The majority of CMIP3 models simulate little change (-5% to 5%) in wet season rainfall by 2030, however by 2090 under the A2 (high) emissions scenario the majority simulate an increase (>5%), with the remainder simulating little change (Table 16.4). There is *moderate* confidence in this range and distribution of possible futures because:

- In simulations of the current climate, the CMIP3 models generally locate the SPCZ in the correct location relative to Vanuatu in the wet season (Brown et al., 2011).
- The CMIP3 models are unable to resolve many of the physical processes involved in producing rainfall. As a consequence, they do not simulate rainfall as well as other variables such as temperature (Volume 1, Chapter 5).

Dry Season (May–October)

Dry season rainfall is projected to decrease over the course of the 21st century. There is *moderate* confidence in this direction of change because:

- Approximately half of the CMIP3 models agree on this direction of change by 2090.

The majority of CMIP3 models simulate little change (-5% to 5%) in dry season rainfall by 2030, however by 2090 they tend to be approximately equally divided between a decrease (<-5%) and little change, with only a few models simulating an increase (>5%) (Table 16.4). There is *low* confidence in this range and distribution of possible futures because:

- In simulations of the current climate, some CMIP3 models have an SPCZ that extends too far east during the dry season, with too much rainfall over Vanuatu (Brown et al., 2011).
- The CMIP3 models are unable to resolve many of the physical processes involved in producing rainfall.

Annual

Total annual rainfall is projected to increase over the course of the 21st century. There is *low* confidence in this direction of change because:

- Projections of annual mean rainfall tend to be equally divided between an increase (>5%) and little change (-5% to 5%) by 2090, with only a few models simulating a decrease (<-5%).
- There is only moderate and low confidence in the range and distribution of wet and dry season rainfall projections respectively, as discussed above.

Interannual variability in rainfall over Vanuatu is strongly influenced by ENSO in the current climate, via the movement of the SPCZ (Volume 1, Section 5.5). As there is no consistency in projections of future ENSO activity (Volume 1, Section 6.4.1), it is not possible to determine whether interannual variability in rainfall will change in the future.

16.7.3 Extremes

Temperature

The intensity and frequency of days of extreme heat are projected to increase over the course of the 21st century. There is *very high* confidence in this direction of change because:

- An increase in the intensity and frequency of days of extreme heat is physically consistent with rising greenhouse gas concentrations.
- All CMIP3 models agree on the direction of change for both intensity and frequency.

The majority of CMIP3 models simulate an increase of approximately 1°C in the temperature experienced on the 1-in-20-year hot day by 2055 under the B1 (low) emissions scenario, with an increase of over 2.5°C simulated by the majority of models by 2090 under the A2 (high) emissions scenario (Table 16.4). There is *low* confidence in this range and distribution of possible futures because:

- In simulations of the current climate, the CMIP3 models tend to underestimate the intensity and frequency of days of extreme heat (Volume 1, Section 5.2.4).
- Smaller increases in the frequency of days of extreme heat are projected by the CCAM 60 km simulations.

Rainfall

The intensity and frequency of days of extreme rainfall are projected to increase over the course of the 21st century. There is *high* confidence in this direction of change because:

- An increase in the frequency and intensity of extreme rainfall is consistent with larger-scale projections, based on the physical argument that the atmosphere is able to hold more water vapour in a warmer climate (Allen and Ingram, 2002; IPCC, 2007). It is also consistent with the projected likely increase in the intensity of the SPCZ (Volume 1, Section 6.4.5).

- Almost all of the CMIP3 models agree on this direction of change for both intensity and frequency.

The majority of CMIP3 models simulate an increase of at least 15 mm in the amount of rain received on the 1-in-20-year wet day by 2055 under the B1 (low) emissions scenario, with an increase of at least 25 mm simulated by 2090 under the A2 (high) emissions scenario. The majority of models project that the current 1-in-20-year event will occur, on average, three to four times every year by 2055 under the B1 (low) emissions scenario and four times a year by 2090 under the A2 (high) emissions scenario. There is *low* confidence in this range and distribution of possible futures because:

- In simulations of the current climate, the CMIP3 models tend to underestimate the intensity and frequency of extreme rainfall (Volume 1, Section 5.2.4).
- The CMIP3 models are unable to resolve many of the physical processes involved in producing extreme rainfall.

Drought

Little change is projected in the incidence of drought over the course of the 21st century. There is *low* confidence in this direction of change because:

- There is only low confidence in the range of dry season rainfall projections (Section 16.7.2), which directly influences projections of future drought conditions.

The majority of CMIP3 models project that the frequency of mild drought will remain approximately stable from 2030 throughout the 21st century at seven to eight times every 20 years,

under the B1 (low) and A1B (medium) emissions scenarios. For the A2 (high) emissions scenario, a small decline from eight to nine times every 20 years in 2030 to seven to eight times by 2090 is projected. The frequency of moderate and severe drought is projected to remain approximately stable, at once to twice and once every 20 years, respectively.

Tropical Cyclones

Tropical cyclone numbers are projected to decline in the south-west Pacific Ocean basin (0–40°S, 130°E–170°E) over the course of the 21st century. There is *moderate* confidence in this direction of change because:

- Many studies suggest a decline in tropical cyclone frequency globally (Knutson et al., 2010).
- Tropical cyclone numbers decline in the south-west Pacific Ocean in the majority assessment techniques.

Based on the direct detection methodologies (Curvature Vorticity Parameter (CVP) and the CSIRO Direct Detection Scheme (CDD) described in Volume 1, Section 4.8.2), 55% of projections show no change or a decrease in tropical cyclone formation when applied to the CMIP3 climate models for which suitable output is available. When these techniques are applied to CCAM, 100% of projections show a decrease in tropical cyclone formation. In addition, the Genesis Potential Index (GPI) empirical technique suggests that conditions for tropical cyclone formation will become less favourable in the south-west Pacific Ocean basin, for the majority (80%) of analysed CMIP3 models. There is *moderate* confidence in this range and distribution of possible futures because in simulations of the

current climate, the CVP, CDD and GPI methods capture the frequency of tropical cyclone activity reasonably well (Volume 1, Section 5.4).

Despite this projected reduction in total cyclone numbers, five of the six CCAM 60 km simulations show an increase in the proportion of the most severe cyclones. This increase in wind hazard coincides with a poleward shift in the latitude at which tropical cyclones are most intense. Most models also indicate a reduction in tropical cyclone wind hazard north of 20°S latitude.

16.7.4 Ocean Acidification

The acidification of the ocean will continue to increase over the course of the 21st century. There is *very high* confidence in this projection as the rate of ocean acidification is driven primarily by the increasing oceanic uptake of carbon dioxide, in response to rising atmospheric carbon dioxide concentrations.

Projections from all analysed CMIP3 models indicate that the annual maximum aragonite saturation state will reach values below 3.5 by about 2035 and continue to decline thereafter (Figure 16.9; Table 16.4). There is *moderate* confidence in this range and distribution of possible futures because the projections are based on climate models without an explicit representation of the carbon cycle and with relatively low resolution and known regional biases.

The impact of acidification change on the health of reef ecosystems is likely to be compounded by other stressors including coral bleaching, storm damage and fishing pressure.

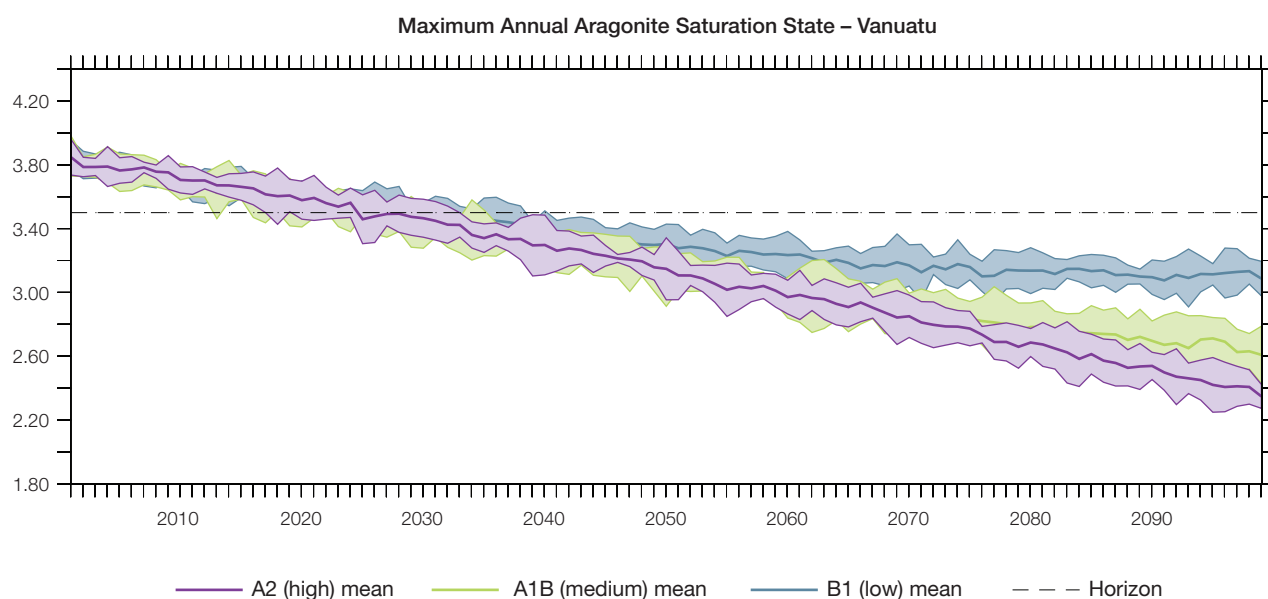


Figure 16.9: Multi-model projections, and their associated uncertainty (shaded area represents two standard deviations), projections of the maximum annual aragonite saturation state in the sea surface waters of the Vanuatu region under the different emissions scenarios. The dashed black line represents an aragonite saturation state of 3.5.

16.7.5 Sea Level

Mean sea level is projected to continue to rise over the course of the 21st century. There is *very high* confidence in this direction of change because:

- Sea-level rise is a physically consistent response to increasing ocean and atmospheric temperatures, due to thermal expansion of the water and the melting of glaciers and ice caps.
- Projections arising from all CMIP3 models agree on this direction of change.

The CMIP3 models simulate a rise of between approximately 5–15 cm by 2030, with increases of 20–60 cm indicated by 2090 under the higher emissions scenarios (i.e. A2 (high) and A1B (medium);

Figure 16.10; Table 16.4). There is *moderate* confidence in this range and distribution of possible futures because:

- There is significant uncertainty surrounding ice-sheet contributions to sea-level rise and a rise larger than projected above cannot be excluded (Meehl et al., 2007b). However, understanding of the processes is currently too limited to provide a best estimate or an upper bound (IPCC, 2007).
- Globally, since the early 1990s, sea level has been rising near the upper end of the above projections. During the 21st century, some studies (using semi-empirical models) project faster rates of sea-level rise.

Interannual variability of sea level will lead to periods of lower and higher regional sea levels. In the past, this interannual variability has been about 18 cm (5–95% range, after removal of the seasonal signal; dashed lines in Figure 16.10 (a)) and it is likely that a similar range will continue through the 21st century. In addition, winds and waves associated with weather phenomena will continue to lead to extreme sea-level events.

In addition to the regional variations in sea level associated with ocean and mass changes, there are ongoing changes in relative sea level associated with changes in surface loading over the last glacial cycle (glacial isostatic adjustment) and local tectonic motions. The glacial isostatic motions are relatively small for the PCCSP region.

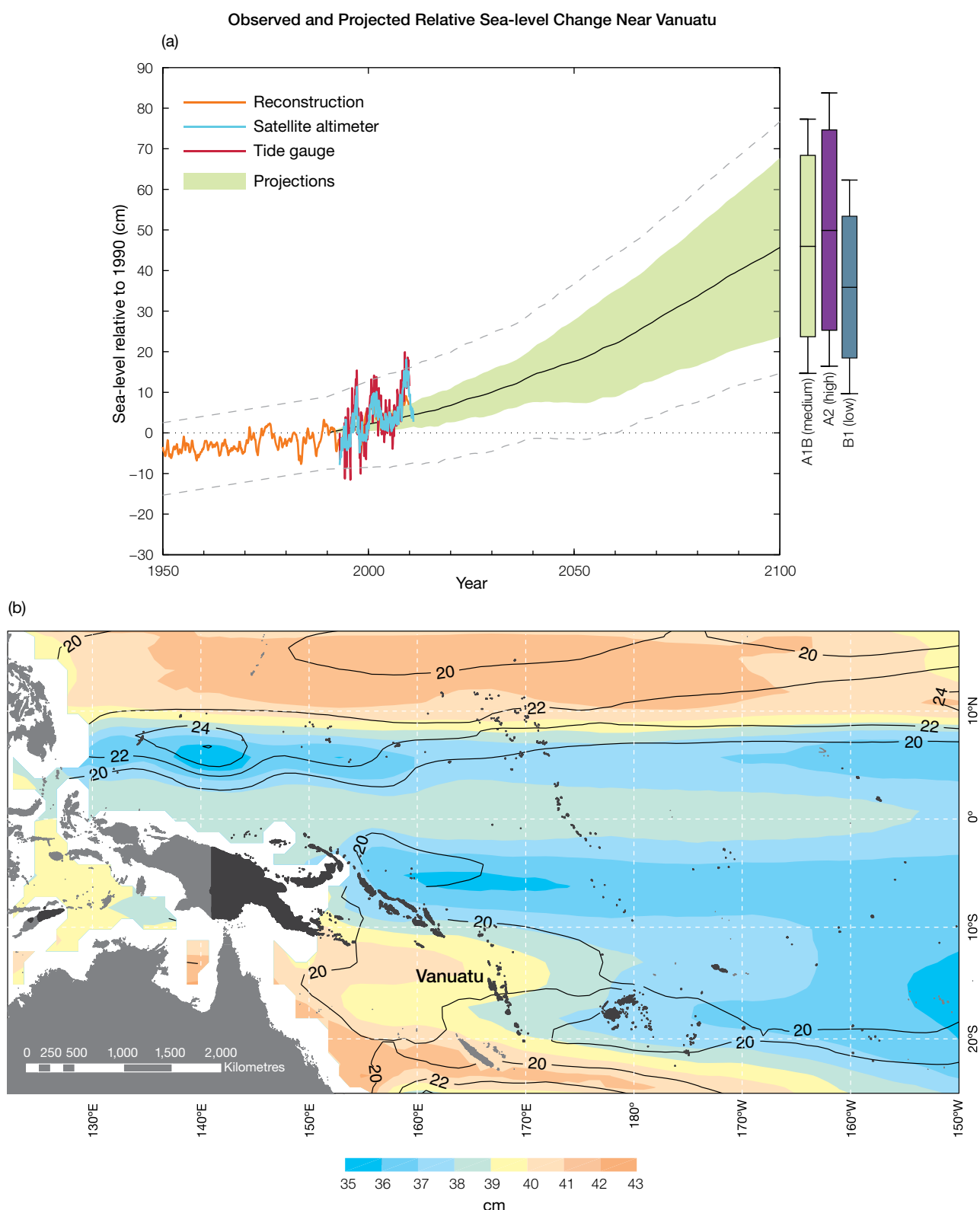


Figure 16.10: Observed and projected relative sea-level change near Vanuatu. (a) The observed in situ relative sea-level records are indicated in red, with the satellite record (since 1993) in light blue. The gridded sea level at Vanuatu (since 1950, from Church and White (in press)) is shown in orange. The projections for the A1B (medium) emissions scenario (5–95% uncertainty range) are shown by the green shaded region from 1990–2100. The range of projections for the B1 (low), A1B (medium) and A2 (high) emissions scenarios are also shown by the bars on the right. The dashed lines are an estimate of interannual variability in sea level (5–95% range about the long-term trends) and indicate that individual monthly averages of sea level can be above or below longer-term averages. (b) The projections (in cm) for the A1B (medium) emissions scenario in the Vanuatu region for the average over 2081–2100 relative to 1981–2000 are indicated by the shading, with the estimated uncertainty in the projections indicated by the contours (in cm).

16.7.6 Projections Summary

The projections presented in Section 16.7 are summarised in Table 16.4. For detailed information regarding the various uncertainties associated with the table values, refer to the preceding text in Sections 16.7 and 1.7, in addition to Chapters 5 and 6 in Volume 1. When interpreting the differences between projections for the B1 (low), A1B (medium) and A2 (high) emissions scenarios, it is also important to consider the emissions pathways associated with each scenario (Volume 1, Figure 4.1) and the fact that a slightly different subset of models was available for each (Volume 1, Appendix 1).

Table 16.4: Projected change in the annual and seasonal-mean climate for Vanuatu, under the B1 (low; blue), A1B (medium; green) and A2 (high; purple) emissions scenarios. Projections are given for three 20-year periods centred on 2030 (2020–2039), 2055 (2046–2065) and 2090 (2080–2099), relative to 1990 (1980–1999). Values represent the multi-model mean change \pm twice the inter-model standard deviation (representing approximately 95% of the range of model projections), except for sea level where the estimated mean change and the 5–95% range are given (as they are derived directly from the Intergovernmental Panel on Climate Change Fourth Assessment Report values). The confidence (Section 1.7.2) associated with the range and distribution of the projections is also given (indicated by the standard deviation and multi-model mean, respectively). See Volume 1, Appendix 1 for a complete listing of CMIP3 models used to derive these projections.

Variable	Season	2030	2055	2090	Confidence
Surface air temperature (°C)	Annual	+0.6 \pm 0.4 +0.7 \pm 0.4 +0.7 \pm 0.3	+1.0 \pm 0.5 +1.4 \pm 0.6 +1.4 \pm 0.3	+1.4 \pm 0.7 +2.2 \pm 0.9 +2.6 \pm 0.6	High
Maximum temperature (°C)	1-in-20-year event	N/A	+1.0 \pm 0.6 +1.5 \pm 0.7 +1.5 \pm 0.5	+1.3 \pm 0.5 +2.1 \pm 0.9 +2.6 \pm 1.2	Low
Minimum temperature (°C)	1-in-20-year event	N/A	+1.2 \pm 1.8 +1.5 \pm 1.9 +1.5 \pm 1.7	+1.5 \pm 1.8 +2.0 \pm 1.9 +2.3 \pm 1.8	Low
Total rainfall (%)*	Annual	+3 \pm 9 +2 \pm 11 +1 \pm 17	+1 \pm 12 +3 \pm 15 +3 \pm 16	+1 \pm 16 +3 \pm 19 +8 \pm 20	Low
Wet season rainfall (%)*	November-April	+5 \pm 8 +3 \pm 11 +3 \pm 17	+3 \pm 12 +5 \pm 15 +5 \pm 15	+3 \pm 15 +7 \pm 19 +11 \pm 18	Moderate
Dry season rainfall (%)*	May-October	0 \pm 16 +1 \pm 20 -2 \pm 22	-4 \pm 20 -1 \pm 24 -1 \pm 27	-2 \pm 23 -4 \pm 25 +2 \pm 31	Low
Sea-surface temperature (°C)	Annual	+0.6 \pm 0.4 +0.6 \pm 0.3 + 0.6 \pm 0.4	+0.9 \pm 0.5 +1.2 \pm 0.5 +1.3 \pm 0.4	+1.3 \pm 0.5 +2.0 \pm 0.7 +2.5 \pm 0.6	High
Aragonite saturation state (Ω_{ar})	Annual maximum	+3.5 \pm 0.1 +3.4 \pm 0.1 +3.4 \pm 0.1	+3.2 \pm 0.1 +3.0 \pm 0.1 +3.0 \pm 0.1	+3.1 \pm 0.1 +2.6 \pm 0.1 +2.5 \pm 0.1	Moderate
Mean sea level (cm)	Annual	+10 (5–16) +10 (5–16) +10 (3–17)	+19 (10–27) +20 (8–31) +19 (7–31)	+32 (17–47) +40 (20–59) +42 (21–63)	Moderate

*The MIROC3.2(medres) and MIROC3.2(hires) models were eliminated in calculating the rainfall projections, due to their inability to accurately simulate present-day activity of the South Pacific Convergence Zone (Volume 1, Section 5.5.1).